iScience

Article

Homoporous polydimethylsiloxane membrane microfilter for ultrafast label-free isolation and recognition of circulating tumor cells in peripheral blood

Peng Xie, Xiaoyue Yao, Zhenyu Chu, ..., Haodong Tang, Jiahua Zhou, Wanqin Jin

zhoujh@seu.edu.cn (J.Z.)
wqjin@njtech.edu.cn (W.J.)

Highlights

Our prepared PDMS membrane is homoporous

Owning ultrahigh porosity

Our membranes have been proved to have a high pure water flux

Low-cost and efficient strategy without any support of bulky equipment

CellPress
OPEN ACCESS

Article

Homoporous polydimethylsiloxane membrane microfilter for ultrafast label-free isolation and recognition of circulating tumor cells in peripheral blood

Peng Xie,[1] Xiaoyue Yao,[2] Zhenyu Chu,[2] Yang Yang,[3] Haifeng Li,[1] Siyuan Tan,[1] Haodong Tang,[1] Jiahua Zhou,[3,4,*] and Wanqin Jin[2,*]

SUMMARY

The detection of circulating tumor cells (CTCs) in peripheral blood is a novel and accurate technique for the early diagnosis of cancers. However, this method is challenging because of the need for high collection efficiency due to the ultralow content and similar size of CTCs compared with other blood cells. To address the aforementioned issue, we proposed a homoporous polydimethylsiloxane (PDMS) membrane and its microfilter device to perform the ultrafast isolation and identification of CTCs directly from peripheral blood without any labeling treatment. The membrane pores can be homogenously controlled at a size of 6.3 μm through the cross-linking time of PDMS during a filtration-coating strategy. Within only 10 s, the designed device achieved a retention rate greater than 70% for pancreatic cancer cells, and it exhibited excellent cell compatibility to support cell proliferation. The isolated CTCs on this membrane can be easily observed and identified using a fluorescence microscope.

INTRODUCTION

Circulating tumor cells (CTCs) are cancer cells that shed from primary or metastatic tumor lesions to enter the peripheral blood or lymphatic circulation, which can spread and cause tumor metastasis.[1] CTCs can serve as an essential assay target for the diagnosis of primary tumors. Compared with tissue biopsy, the liquid biopsy to detect CTCs is minimally invasive and can be used for the early diagnosis of cancers, providing risk prediction of tumor progression, metastasis, and recurrence, along with evaluation of chemotherapy or radiotherapy effects, indicators of individual sensitivity to antitumor drugs, and determination of treatment targets.[2–8] The isolation, enumeration, and molecular characterization of CTCs enable the establishment of a relationship between cancer biology and individualized/precision therapy. Recent clinical studies have already proven that the enumeration of CTCs in peripheral blood can directly indicate the advancement of various cancers, including metastatic breast,[9,10] colorectal,[11,12] prostate,[13,14] lung,[15–18] and ovarian[19] cancer. However, this novel diagnostic technique suffers from a major challenge in the efficient collection of enough CTCs from low volumes of blood samples because 1 mL of peripheral blood from metastatic tumor patients contains fewer than 10 CTCs, which makes the precise separation of CTCs from numerous hematological cells difficult.[20,21]

In the last decade, many new techniques for CTC separation have emerged in the pursuit of greater precision and speed without damage to CTCs. Two categories of methods can achieve this purpose, namely, affinity-based isolation strategies and physical capture strategies. Affinity-based isolation relies on establishing an affinity interface to specifically adsorb CTCs. Magnetic beads,[22] red blood cell affinity interfaces modified with antibodies (RBC-Ab),[23] microfluidic chips,[21] and microfluidic platforms[24] are typical routes to isolate CTCs from other cells in blood. The key to this technology relies on the expression of epithelial cell markers such as epithelial cell adhesion molecule (EpCAM). However, epithelial markers are easily lost during the complex epithelial-mesenchymal transition (EMT), which is a crucial step in the metastatic process. EpCAM may also be found in healthy individuals, which interferes with the detection accuracy; moreover, certain tumor types, such as melanoma and leukemia, are not of epithelial origin. Therefore, all of the aforementioned limitations have hampered the practical isolation and detection of CTCs. In contrast, the capture strategy without specific ligand binding, known as "physical capture," mainly relies on the distinct physical properties of CTCs (cell size,[2,3,21,25–27] cell density,[28,29] electrical properties,[30] etc.) to realize their specific separation. Membrane separation is one of the latest techniques employed in this field, based on the principle of size sieving. The ScreenCell (Paris, France) membrane device is the only product that currently enables the isolation and detection of CTCs from peripheral blood for biological research on cancer.[25] However, its high cost and low separation accuracy

[1]Department of Hepatopancreatobiliary Surgery, Zhongda Hospital, School of Medicine, Southeast University, Nanjing, Jiangsu Province 210009, China
[2]State Key Laboratory of Materials–Oriented Chemical Engineering, College of Chemical Engineering, Nanjing Tech University, Nanjing 211816, P.R. China
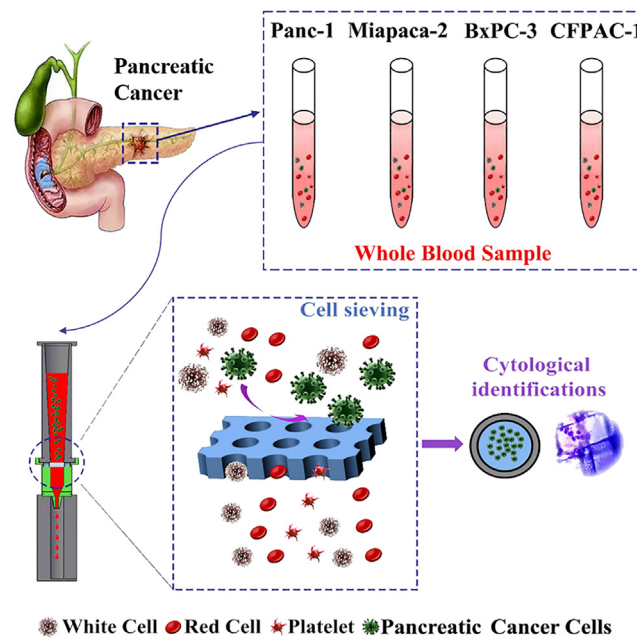[3]Department of Hepatopancreatobiliary Surgery, Zhongda Hospital Southeast University, Nanjing, Jiangsu Province 210009, China
[4]Lead contact
*Correspondence: zhoujh@seu.edu.cn (J.Z.), wqjin@njtech.edu.cn (W.J.)

Figure 1. Schematic illustration of the detection of CTCs from peripheral blood with the microfiltration device integrated with a PDMS filter membrane

strongly limit its popularization in the early detection of cancer cells and rapid evaluation of treatment effects. In addition, the membrane in this device presents low porosity and biocompatibility, with many overlapping pores, and therefore shows unsatisfactory separation ability. Low separation flux and easy cell damage greatly reduce the capture efficiency, which may cause the failure of cancer diagnosis using this method. Hence, it is desirable to design a cell-friendly membrane with high porosity, greatly improving the rejection efficiency and precision using as little blood as possible.

In this work, we have proposed a homoporous polydimethylsiloxane (PDMS) membrane with ultrahigh porosity along with a handheld device to perform fast, nondamaging, and label-free CTC separation and recognition in peripheral blood.[31] The membrane was constructed through a vacuum filtration method to exactly control the pore size from 2 to 15 μm, accurately matching different kinds of tumor cells. A schematic of the microfilter device integrated with the PDMS filter membrane is shown in Figure 1. Cytotoxicity testing of this membrane confirmed that this membrane caused little damage to four different tumor cells (Panc-1, Miapaca-2, BxPC-3, and CFPAC-1), exhibiting excellent biocompatibility. Then, an easily sterilized and reusable device was designed to install the as-prepared membrane, simplifying the operations of blood separation and CTC collection. Using four tumor cell lines derived from pancreatic cancer as targets, more than 70% of CTCs were obtained from only a 1 mL peripheral blood sample within 10 s (approximately 65–81 were separated when 100 cancer cells were spiked into 1 mL peripheral blood samples in repeated experiments). This cell-oriented membrane device is promising for providing a highly effective and minimally invasive technique for CTC capture for the clinical diagnosis of cancers.

RESULTS AND DISCUSSION

Pore structure of the PDMS membranes

Among various cells in patients' blood containing CTCs, the size of CTCs, which is generally 10–30 μm, is much higher than that of red blood cells (6–8 μm) and platelets (2–3 μm). Hence, to precisely capture CTCs, the pore size must be lower than but close to 8 μm, which can be expected to obtain both high separation selection and flux. Here, PDMS was selected as the target membrane material due to its excellent chemical stability, biocompatibility, and few functional groups, preventing interactions that damage cells. PDMS has been confirmed as a blood-compatible material for broad application in cell culture, drug delivery, and wound healing. The flexibility, biocompatibility, nontoxicity, good stability, and high transparency make PDMS an advantageous candidate for the material selection of microfiltration membranes.[8,32,33,34] For comparison, three preparation methods were designed to study the membrane formation process controlled by the cross-linking period. As shown in Figure 2A, the dip-coating strategy can easily create a PDMS layer on the nylon fibers. However, due to the viscous PDMS, the inner cavities were almost filled to produce dead pores without any separation channels. In contrast, the spin-coating approach easily produced a membrane only on the surface of the substrate instead of hole filling, resulting from centrifugal force. In this case, a dense and thick PDMS layer covered the whole substrate surface to present no pore structure. Using the filtration-coating route, a PDMS layer enables modification of only the substrate fibers to reduce the pore size instead of filling the pores (Figure 2B). This is because under a vacuum force, the redundant PDMS bound only weakly to the substrate will be pumped away to retain the pore structure.
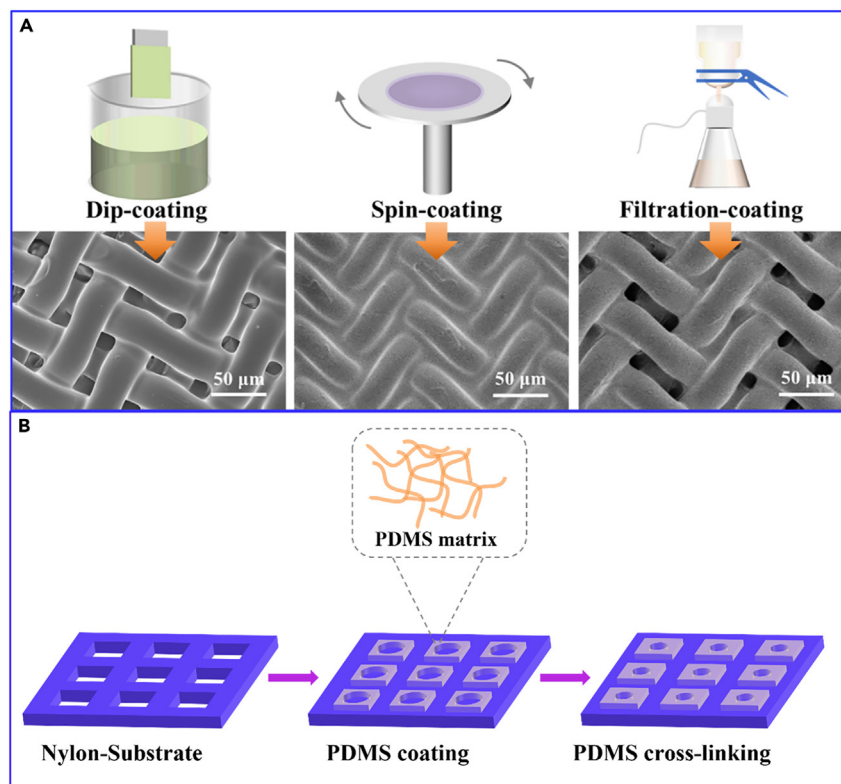
Figure 2. Schematic drawing of different preparation methods of PDMS membrane
(A) Membrane morphologies using different preparation methods, including dip-coating, spin-coating, and filtration-coating.
(B) Schematic of filtration-coating method.

Because PDMS continuously undergoes cross-linking to increase the molecular weight and form denser networks, the cross-linking period directly determines the viscosity of the casting solution, which affects the membrane properties. Figures 3A–3F show the bare substrate and the morphologies of membranes prepared with different cross-linking times from 4 to 7 h. Overall, the pore size gradually decreased with prolonged time. The average pore sizes of these membranes were 22.0, 18.3, 15.6, 10.9, and 6.3 μm for 4, 5, 6, 6.5, and 7 h, respectively. Hence, the PDMS membrane in Figure 3F can satisfy the pore size requirement for CTC isolation in blood. Subsequently, the pure water fluxes of these membranes were investigated to identify the influence of the pore size.

As shown in Figure 4A, the viscosity of the casting solution can be adjusted from 16.2 to 136.8 cP to prepare the above membranes with different fluxes. There is an evident decrease in the water flux after the coating of the PDMS membrane, and this decrease occurs rapidly with the increase in viscosity corresponding to the reduction in the membrane pore size (Figure 4B). The average water fluxes of these membranes are 78.4, 73.2, 71.6, 58.4, and 44.8 mL/(min·cm^{-2}) for pore sizes of 22.0, 18.3, 15.6, 10.9, and 6.3 μm, respectively. Moreover, during continuous drawing through 0.1 MPa, the as-prepared membrane with 6.3 μm pores maintained a stable flux, indicating satisfactory adhesion on the nylon substrate without obvious damage. Then, we compared the FTIR spectrum of this PDMS membrane and the bare substrate to reveal three extra peaks belonging to PDMS. In contrast to the nylon substrate, the characteristic peaks located at 800 cm^{-1}, 2965 cm^{-1}, 1266 cm^{-1}, and 1015 cm^{-1} belonged to the asymmetric stretching vibration of CH$_3$[35] (Figure 4C). The stretching vibration of CH$_3$-Si and the asymmetric stretching vibration of Si-O-Si confirmed that a solid PDMS coating had been formed on the nylon substrate. Furthermore, according to the XRD patterns in Figure 4D, a wide diffraction peak at 2θ = 12° indicated the amorphous crystalline structure of PDMS. The XPS results of C1s orbits also showed C-Si bonds from PDMS chains and C-C bonds from both PDMS and the nylon substrate. To obtain a stable separation performance, the desired membrane should have a negative charge, which enables the electrostatic repulsion of most proteins and red blood cells, which have negatively charged membranes. This repulsion can prevent the blocking of membrane pores, which may greatly affect the permeation. Our prepared membrane has been proven to possess an overall negatively charged surface when the pH is higher than 3.47. Especially between pH 7.35 and 7.45, which is the normal environment of blood, this membrane shows a strong charge of ca. −78.4 mV, promoting resistance to membrane fouling by proteins and cells.

Design of a handheld membrane microfilter

For the further identification of tumor cells after blood separation, the cell compatibility of the membrane is essential to ensure cell morphology and activity. Therefore, four types of pancreatic cancer cells (Panc-1, Miapaca-2, BxPC-3, and CFPAC-1) were
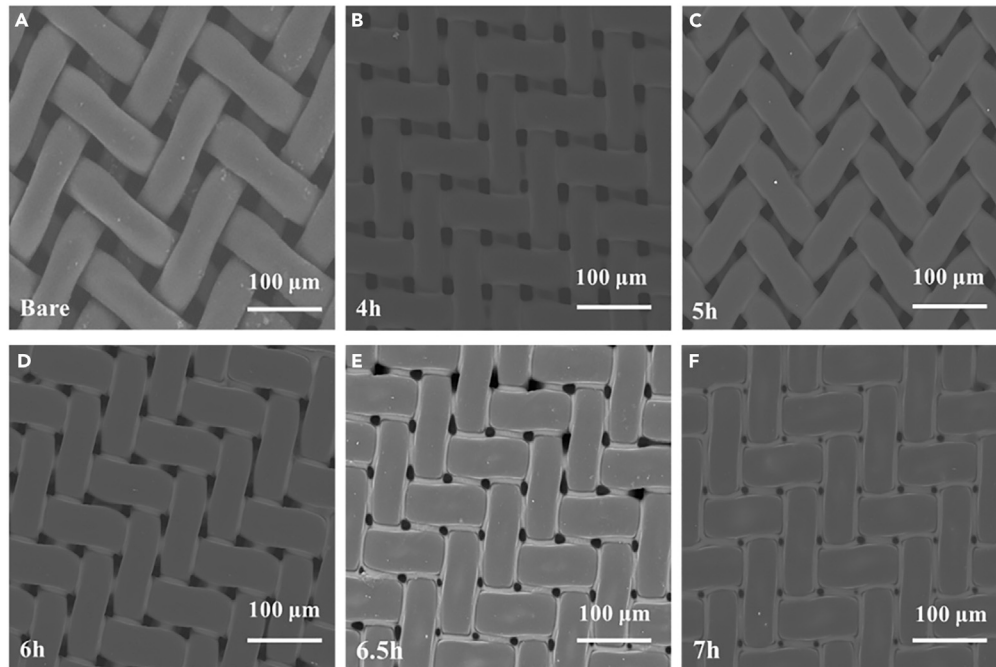
Figure 3. Membrane pore structure at different time
(A–F) FESEM images of the bare substrate and membranes prepared with different cross-linking times from 4 to 7 h.

cultured to perform the CCK-8 assay to examine the toxicity of the membrane to tumor cells. As shown in Figure 5, the proliferation rates of these cells on the PDMS membrane are basically consistent with those of the control groups (p > 0.05) using free growth. This evidence verifies that the PDMS membrane has remarkable biocompatibility with cells, showing little influence on proliferation, and can thus protect the activity and integrity of the tumor cells for the final analysis of the cell morphology and pathology.

To realize practical CTC separation from whole blood, a microfilter device (Figure 6A) was designed to take advantage of the characteristics of the prepared PDMS membrane (Figure 6B). This device is composed of two core modules to integrate together. The upper part of the microfilter is designed to contain 7 mL whole blood samples in its tube, and the lower part loads a syringe needle enabled to connect with a collection tube to produce vacuum force for the blood separation. The PDMS membrane will be fixed and sealed between the two parts mentioned earlier to benefit membrane replacement. It can be observed in Figure 6C that within only 10 s, human blood can be sieved into the collection tube (with EDTA as the anticoagulant), indicating excellent efficiency.

Isolation performance of the membrane microfilter device

A suspension of human peripheral blood carrying a known number of various tumor cells was introduced into the filtration device to perform the separation operation. To differentiate tumor cells from leukocytes, we introduced two dyes that can specifically recognize leukocytes and epithelial tumor cells. Figure 7 shows images of cells captured on the membrane under a fluorescence microscopy. We found that although CTCs were extremely rare in blood, they were unable to pass through these membrane pores and were trapped on the membrane surface because they were larger than the pore size. Additionally, these images revealed the presence of specific immunophenotypes in epithelial-marker-positive tumor cells. Although some leukocytes were retained on the filter membrane, cell counting was relatively easy because the individual cells had already been captured and dispersed on the membrane. This microfilter is also applicable to four kinds of pancreatic cancer cells with different sizes.

We further tested the isolation efficiency of the microfilter for four human pancreatic cancer cell lines, Panc-1, Miapaca-2, BxPC-3, and CFPAC-1, presenting different size ranges (Figure 8A). The heterogeneous distribution of each type of cancer cell will create difficulty in the selection of a suitable membrane pore size. Therefore, the membranes with different pore sizes prepared earlier were examined to determine their isolation efficiencies for these cells. As shown in Figure 8B, for Panc-1 and BxPC-3, there are rare differences in the rejection rates among the membrane pore sizes of 15.6, 10.9, and 6.3 μm. However, the 6.3 μm membrane pores were confirmed to exhibit much better isolation performance during the separation of Miapaca-2 and CFPAC-1 cells from whole blood. In this case, this membrane was selected as the optimum separating core in the fabrication of the microfilter device. To clarify that the membrane function differed from that of the substrate, the separation behaviors of the membrane and substrate are compared in Figure 8C. As a result, the substrate rejects less than 20% of the four pancreatic cancer cells, and the superior PDMS membrane enables a general increase in this rate to 64%–78%, illustrating
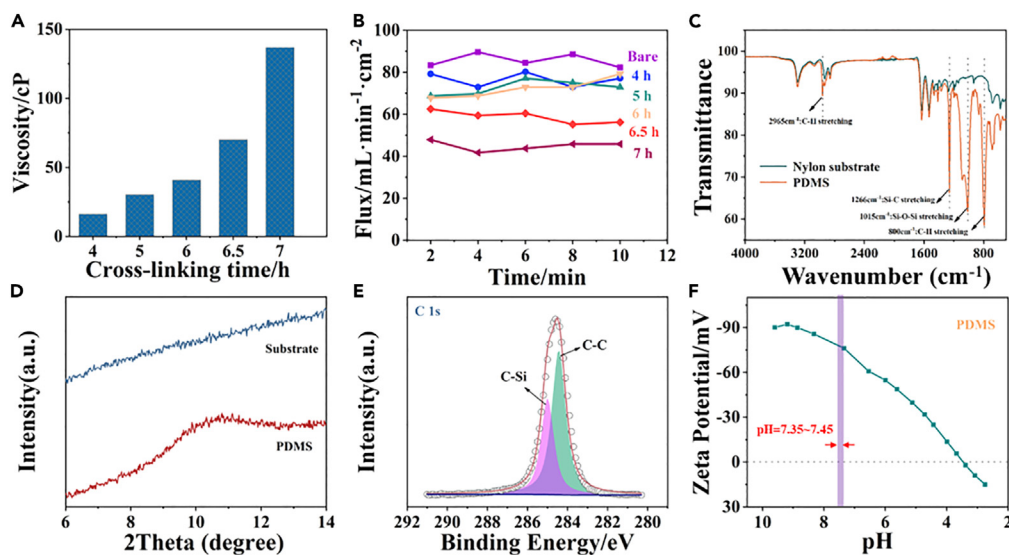
Figure 4. Characterization of the PDMS membrane
(A) The viscosities of the casting solutions with varying cross-linking times.
(B) The pure water fluxes of the PDMS membrane prepared by the above casting solutions.
(C) and (D) FTIR and XRD patterns of the nylon substrate before and after deposition of the PDMS membrane.
(E) XPS image of C1s belonging to the PDMS membrane.
(F) Z-potential characteristics of the PDMS membrane at different pH values.

the superior sieving ability of the PDMS membrane. Interestingly, the other membranes with pore sizes larger than 15.6 μm also presented much better performance than the bare nylon substrate.

Morphological identification of CTCs

To assess the detection sensitivity of the device, the aforementioned four tumor cell lines were preliminarily stained with a nuclear dye, 4,6-diamidino-2-phenylindole (DAPI; Beyotime Institute of Biotechnology, USA), at 37°C for 30 min. Subsequently, these cells were spiked into PBS at 20, 40, 60, 80, and 100 cells/mL, detected by the filter device, and counted under a fluorescence microscope (Figures 9A–9D). The results in Figure 8D show that the capture efficiency remained nearly constant and exceeded 70% when 20–100 tumor cells were present per PBS. Regression analysis of the number of observed tumor cells versus the number of predetermined tumor cells showed that the slopes for Panc-1, Miapaca-2, BxPC-3, and CFPAC-1 were 0.866, 0.835, 0.760, and 0.843, respectively. It was proven that the capture efficiency of the filtration device was not affected by the number of cells added to the test sample and that the tests were reproducible.

The isolated CTCs were identified morphologically by hematoxylin and eosin (H&E) staining. Isolated nonhematological circulating cells with malignant features were defined as CTCs, morphologically identified, and enumerated according to the following criteria: (1) high nuclear-to-cytoplasmic (N/C) ratio; (2) enlarged nuclei, nuclear atypia, and lobulated nuclei; (3) irregular nuclear borders; (4) nuclear hyperchromasia; and (5) high nuclear basophilia.[36] CTMs were defined as clusters formed by ≥ 3 CTCs[37] (Figures 9E–9H). It can be clearly seen from FESEM images (Figures 9I–9L) that the tumor cells were isolated around the membrane pores and that the tumor cells were significantly larger than the membrane pores. Clusters of tumor cells could also be observed on the membrane.

Conclusions

In this study, we successfully designed an ultrasensitive handheld membrane-based microfilter device for the isolation and identification of CTCs in peripheral blood. Although the application of some PDMS membranes in CTC separation has been reported,[32,34] their preparation methods were not capable of large-scale fabrication, or their pores were not uniform enough to achieve a high blood flux combined with a high separation precision. In this work, we designed a vacuum-filtration-coating method for the *in situ* synthesis of PDMS membranes, a low-cost and efficient strategy requiring no bulky equipment. Compared with commercial membranes, the as-prepared membrane exhibits better rejection performance due to its uniform pore structure. Relying on the homogeneous micropores of the PDMS membrane, four kinds of human pancreatic cancer cells can be efficiently captured on the membrane surface within only 10 s. Importantly, the excellent biocompatibility of this membrane prevents damage to the cell activity and morphology, supporting further cell proliferation during the separation process. This portable device can separate viable CTCs from whole blood without prelabeling or processing of samples, resulting in increased cell activity and separation purity. This device holds promise as an inexpensive, efficient, and user-friendly tool that can help generalize the study of CTCs in cancer metastasis and establish their clinical utility as a prognostic marker for the treatment of the disease.
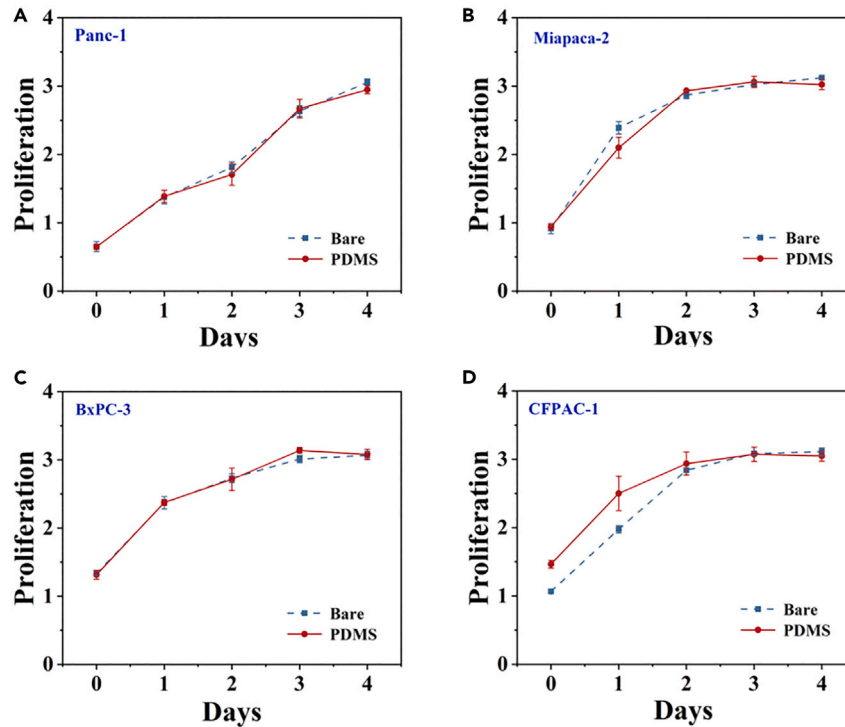
Figure 5. Proliferation changes of the four kinds of pancreatic cancer cells using the CCK-8 assay
(A) Proliferation changes of Panc-1.
(B) Proliferation changes of Miapaca-2.
(C) Proliferation changes of BxPC-3.
(D) Proliferation changes of CFPAC-1.

Limitations of the study

As the central component of the microfiltration device, the limited transparency of the PDMS filter membrane has been found to have a discernible impact on subsequent experimental analyses. Additionally, the application of this microfiltration device in actual clinical settings has not been effectively advanced due to factors such as experimental duration and conditions.
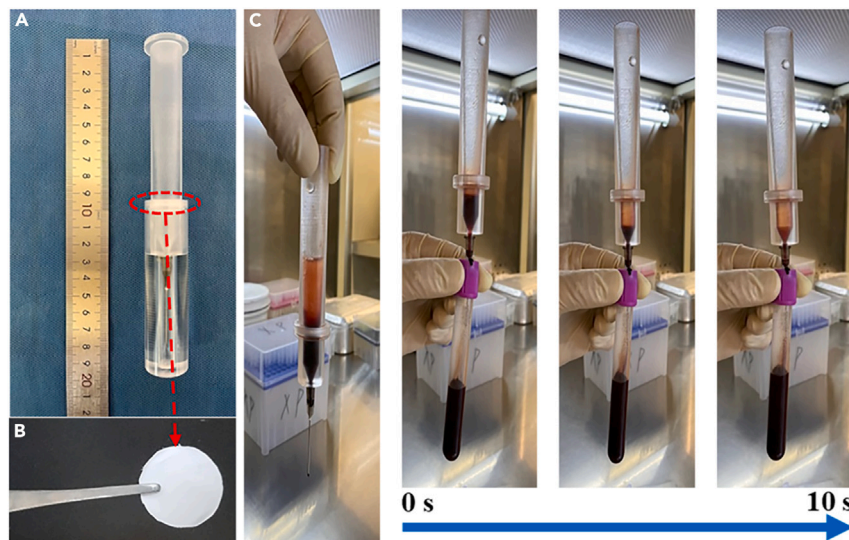
Figure 6. The PDMS membrane-based microfilter
The proposed handheld PDMS membrane (B)-based microfilter (A) for the rapid isolation of CTCs from whole blood (C).
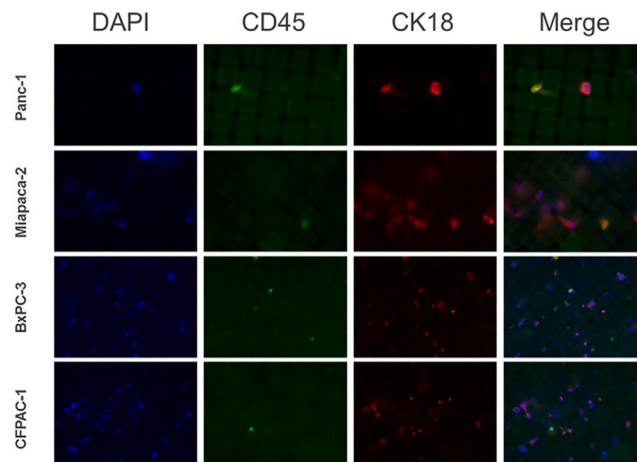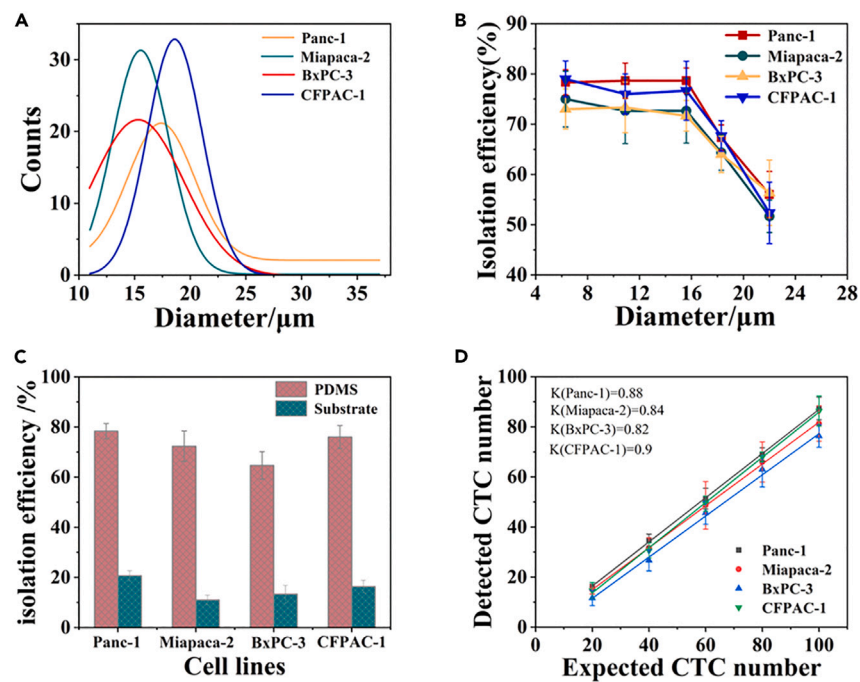
Figure 7. Immunofluorescence images of cells isolated from peripheral blood using the designed membrane microfilter

STAR★METHODS

Detailed methods are provided in the online version of this paper and include the following:

- KEY RESOURCES TABLE
- RESOURCE AVAILABILITY
  - Lead contact
  - Materials availability
  - Data and code availability

Figure 8. Isolation performance of the membrane microfilter device
(A) Size distribution of the applied four kinds of human pancreatic cancer cells.
(B) Isolation efficiencies of the prepared PDMS membrane with different pore sizes.
(C) Comparison of the isolation efficiencies of the PDMS membrane possessing 6.3 μm pores and bare nylon substrate.
(D) Regression analysis of capture efficiency of the PDMS membrane for Panc-1, Miapaca-2, BxPC-3, and CFPAC-1 cells.
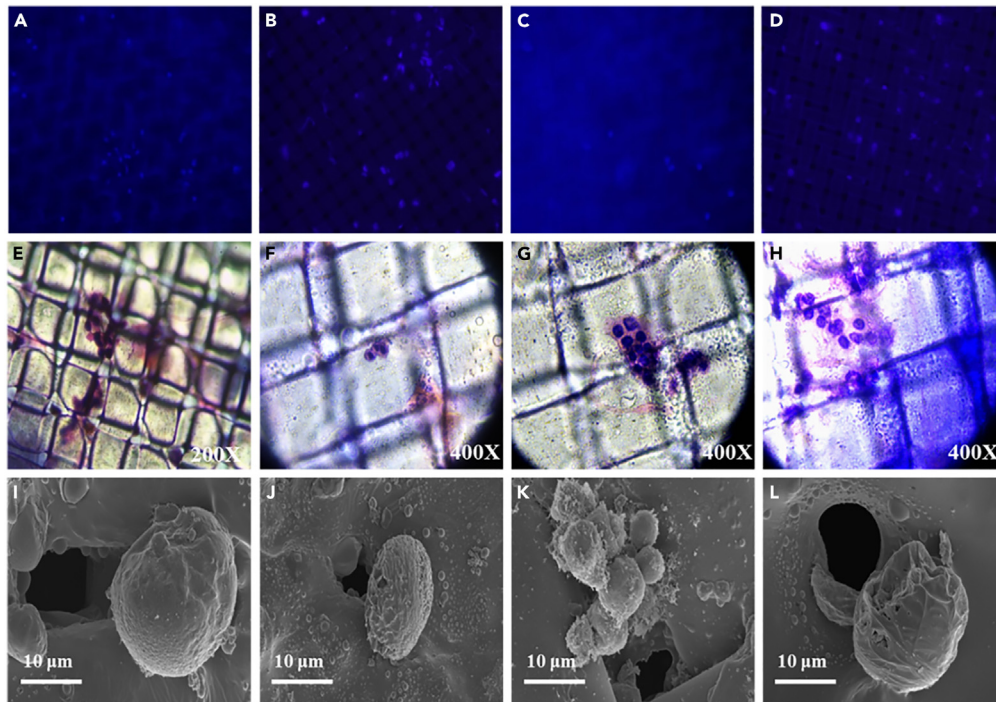
Figure 9. Morphological identification of CTCs

(A–D) Cells preliminarily stained with DAPI were retained on the membrane after filtration.

(E–H) Morphological identifications of the CTCs after separation. (I–L) FESEM images of the captured CTCs on the PDMS filter membrane.

- EXPERIMENTAL MODEL AND SUBJECT DETAILS
  - Ethics statement
  - Chemical reagents and cell culture
  - Preparation of homoporous PDMS membranes
  - Cell separation
- METHOD DETAILS
  - Cell counting kit-8 (CCK-8) assay
  - Identification of the isolated CTCs
- QUANTIFICATION AND STATISTICAL ANALYSIS

SUPPLEMENTAL INFORMATION

Supplemental information can be found online at https://doi.org/10.1016/j.isci.2023.108246.

ACKNOWLEDGMENTS

AUTHOR CONTRIBUTIONS

Conception and design of the study: J.Z. and W.J.. Collection of data, data analysis, and interpretation: P.X., X.Y., Y.Y., H.L., S.T., and H.T.. Drafting of the manuscript: P.X. and X.Y.. Critical revision of the manuscript for important intellectual content: P.X. and Z.C. All authors have read and agreed to the submission of the manuscript.

DECLARATION OF INTERESTS

The authors declare no competing interests.

REFERENCES

1. Deng, Z., Wu, S., Wang, Y., and Shi, D. (2022). Circulating tumor cell isolation for cancer diagnosis and prognosis. EBioMedicine *83*, 104237. https://doi.org/10.1016/j.ebiom.2022.104237.

2. Kamińska, A., Szymborski, T., Witkowska, E., Kijeńska-Gawrońska, E., Świeszkowski, W., Niciński, K., Trzcińska-Danielewicz, J., and Girstun, A. (2019). Detection of circulating tumor cells using membrane-based sers platform: a new diagnostic approach for 'liquid biopsy'. Nanomaterials *9*, 366. https://doi.org/10.3390/nano9030366.

3. Kim, Y.J., Koo, G.B., Lee, J.Y., Moon, H.S., Kim, D.G., Lee, D.G., Lee, J.Y., Oh, J.H., Park, J.M., Kim, M.S., et al. (2014). A microchip filter device incorporating slit arrays and 3-D flow for detection of circulating tumor cells using cav1-epcam conjugated microbeads. Biomaterials *35*, 7501–7510. https://doi.org/10.1016/j.biomaterials.2014.05.039.

4. Chemi, F., Rothwell, D.G., Mcgranahan, N., Gulati, S., Abbosh, C., Pearce, S.P., Zhou, C., Wilson, G.A., Jamal-Hanjani, M., Birkbak, N., et al. (2019). Pulmonary venous circulating tumor cell dissemination before tumor resection and disease relapse. Nat. Med. *25*, 1534–1539. https://doi.org/10.1038/s41591-019-0593-1.

5. Pantel, K., and Alix-Panabières, C. (2019). Liquid biopsy and minimal residual disease - latest advances and implications for cure. Nat. Rev. Clin. Oncol. *16*, 409–424. https://doi.org/10.1038/s41571-019-0187-3.

6. Sparano, J., O'Neill, A., Alpaugh, K., Wolff, A.C., Northfelt, D.W., Dang, C.T., Sledge, G.W., and Miller, K.D. (2018). Association of circulating tumor cells with late recurrence of estrogen receptor-positive breast cancer: a secondary analysis of a randomized clinical trial. JAMA Oncol. *4*, 1700–1706. https://doi.org/10.1001/jamaoncol.2018.2574.

7. Shen, H., Liu, L., Yuan, Z., Liu, Q., Li, B., Zhang, M., Tang, H., Zhang, J., and Zhao, S. (2021). Novel cytosensor for accurate detection of circulating tumor cells based on a dual-recognition strategy and bsa@ag@ir metallic-organic nanoclusters. Biosens. Bioelectron. *179*, 113102. https://doi.org/10.1016/j.bios.2021.113102.

8. Sun, Y., Wu, G., Cheng, K.S., Chen, A., Neoh, K.H., Chen, S., Tang, Z., Lee, P.F., Dai, M., and Han, R.P.S. (2019). CTC phenotyping for a preoperative assessment of tumor metastasis and overall survival of pancreatic ductal adenocarcinoma patients. EBioMedicine *46*, 133–149. https://doi.org/10.1016/j.ebiom.2019.07.044.

9. Cristofanilli, M., Hayes, D.F., Budd, G.T., Ellis, M.J., Stopeck, A., Reuben, J.M., Doyle, G.V., Matera, J., Allard, W.J., Miller, M.C., et al. (2005). Circulating tumor cells: a novel prognostic factor for newly diagnosed metastatic breast cancer. J. Clin. Oncol. *23*, 1420–1430. https://doi.org/10.1200/JCO.2005.08.140.

10. Pachmann, K., Camara, O., Kavallaris, A., Krauspe, S., Malarski, N., Gajda, M., Kroll, T., Jörke, C., Hammer, U., Altendorf-Hofmann, A., et al. (2008). Monitoring the response of circulating epithelial tumor cells to adjuvant chemotherapy in breast cancer allows detection of patients at risk of early relapse. J. Clin. Oncol. *26*, 1208–1215. https://doi.org/10.1200/JCO.2007.13.6523.

11. Wong, S.C.C., Chan, C.M.L., Ma, B.B.Y., Hui, E.P., Ng, S.S.M., Lai, P.B.S., Cheung, M.T., Lo, E.S.F., Chan, A.K.C., Lam, M.Y.Y., et al. (2009). Clinical significance of cytokeratin 20-positive circulating tumor cells detected by a refined immunomagnetic enrichment assay in colorectal cancer patients. Clin. Cancer Res. *15*, 1005–1012. https://doi.org/10.1158/1078-0432.CCR-08-1515.

12. Uen, Y.H., Lu, C.Y., Tsai, H.L., Yu, F.J., Huang, M.Y., Cheng, T.L., Lin, S.R., and Wang, J.Y. (2008). Persistent presence of postoperative circulating tumor cells is a poor prognostic factor for patients with stage i-iii colorectal cancer after curative resection. Ann. Surg Oncol. *15*, 2120–2128. https://doi.org/10.1245/s10434-008-9961-7.

13. Danila, D.C., Heller, G., Gignac, G.A., Gonzalez-Espinoza, R., Anand, A., Tanaka, E., Lilja, H., Schwartz, L., Larson, S., Fleisher, M., and Scher, H.I. (2007). Circulating tumor cell number and prognosis in progressive castration-resistant prostate cancer. Clin. Cancer Res. *13*, 7053–7058. https://doi.org/10.1158/1078-0432.CCR-07-1506.

14. Morgan, T.M., Lange, P.H., Porter, M.P., Lin, D.W., Ellis, W.J., Gallaher, I.S., and Vessella, R.L. (2009). Disseminated tumor cells in prostate cancer patients after radical prostatectomy and without evidence of disease predicts biochemical recurrence. Clin. Cancer Res. *15*, 677–683. https://doi.org/10.1158/1078-0432.CCR-08-1754.

15. Maheswaran, S., Sequist, L.V., Nagrath, S., Ulkus, L., Brannigan, B., Collura, C.V., Inserra, E., Diederichs, S., Iafrate, A.J., Bell, D.W., et al. (2008). Detection of mutations in egfr in circulating lung-cancer cells. N. Engl. J. Med. *359*, 366–377. https://doi.org/10.1056/NEJMoa0800668.

16. Hiltermann, T.J.N., Pore, M.M., van den Berg, A., Timens, W., Boezen, H.M., Liesker, J.J.W., Schouwink, J.H., Wijnands, W.J.A., Kerner, G.S.M.A., Kruyt, F.A.E., et al. (2012). Circulating tumor cells in small-cell lung cancer: a predictive and prognostic factor. Ann. Oncol. *23*, 2937–2942. https://doi.org/10.1093/annonc/mds138.

17. Hou, J.M., Krebs, M.G., Lancashire, L., Sloane, R., Backen, A., Swain, R.K., Priest, L.J.C., Greystoke, A., Zhou, C., Morris, K., et al. (2012). Clinical significance and molecular characteristics of circulating tumor cells and circulating tumor microemboli in patients with small-cell lung cancer. J. Clin. Oncol. *30*, 525–532. https://doi.org/10.1200/JCO.2010.33.3716.

18. Krebs, M.G., Sloane, R., Priest, L., Lancashire, L., Hou, J.M., Greystoke, A., Ward, T.H., Ferraldeschi, R., Hughes, A., Clack, G., et al. (2011). Evaluation and prognostic significance of circulating tumor cells in patients with non-small-cell lung cancer. J. Clin. Oncol. *29*, 1556–1563. https://doi.org/10.1200/JCO.2010.28.7045.

19. Fan, T., Zhao, Q., Chen, J.J., Chen, W.T., and Pearl, M.L. (2009). Clinical significance of circulating tumor cells detected by an invasion assay in peripheral blood of patients with ovarian cancer. Gynecol. Oncol. *112*, 185–191. https://doi.org/10.1016/j.ygyno.2008.09.021.

20. Fan, X., Jia, C., Yang, J., Li, G., Mao, H., Jin, Q., and Zhao, J. (2015). A microfluidic chip integrated with a high-density PDMS-based microfiltration membrane for rapid isolation and detection of circulating tumor cells. Biosens. Bioelectron. *71*, 380–386. https://doi.org/10.1016/j.bios.2015.04.080.

21. Liu, Z., Huang, Y., Liang, W., Bai, J., Feng, H., Fang, Z., Tian, G., Zhu, Y., Zhang, H., Wang, Y., et al. (2021). Cascaded filter deterministic lateral displacement microchips for isolation and molecular analysis of circulating tumor cells and fusion cells. Lab Chip *21*, 2881–2891. https://doi.org/10.1039/d1lc00360g.

22. Chang, Z.M., Zhang, R., Yang, C., Shao, D., Tang, Y., Dong, W.F., and Wang, Z. (2020). Cancer-leukocyte hybrid membrane-cloaked magnetic beads for the ultrasensitive isolation, purification, and non-destructive release of circulating tumor cells. Nanoscale *12*, 19121–19128. https://doi.org/10.1039/d0nr04097e.

23. Shen, H., Su, R., Peng, J., Zhu, L., Deng, K., Niu, Q., Song, Y., Yang, L., Wu, L., Zhu, Z., and Yang, C. (2022). Antibody-engineered red blood cell interface for high-performance capture and release of circulating tumor cells. Bioact. Mater. *11*, 32–40. https://doi.org/10.1016/j.bioactmat.2021.09.034.

24. Wu, L., Ding, H., Qu, X., Shi, X., Yang, J., Huang, M., Zhang, J., Zhang, H., Song, J., Zhu, L., et al. (2020). Fluidic multivalent membrane nanointerface enables synergetic enrichment of circulating tumor cells with high efficiency and viability. J. Am. Chem. Soc. *142*, 4800–4806. https://doi.org/10.1021/jacs.9b13782.

25. Desitter, I., Guerrouahen, B.S., Benali-Furet, N., Wechsler, J., Jänne, P.A., Jänne, P.A., Yanagita, M., Wang, L., Berkowitz, J.A., Distel, R.J., and Cayre, Y.E. (2011). A new device for rapid isolation by size and characterization of rare circulating tumor cells. Anticancer Res. *31*, 427–441.

26. Cima, I., Kong, S.L., Sengupta, D., Tan, I.B., Phyo, W.M., Lee, D., Hu, M., Iliescu, C., Alexander, I., Goh, W.L., et al. (2016). Tumor-derived circulating endothelial cell clusters in colorectal cancer. Sci. Transl. Med. *8*, 345ra89. https://doi.org/10.1126/scitranslmed.aad7369.

27. Lee, H.J., Oh, J.H., Oh, J.M., Park, J.M., Lee, J.G., Kim, M.S., Kim, Y.J., Kang, H.J., Jeong, J., Kim, S.I., et al. (2013). Efficient isolation and accurate in situ analysis of circulating tumor cells using detachable beads and a high-pore-density filter. Angew. Chem. Int. Ed. Engl. *52*, 8337–8340. https://doi.org/10.1002/anie.201302278.

28. Baker, M.K., Mikhitarian, K., Osta, W., Callahan, K., Hoda, R., Brescia, F., Kneuper-Hall, R., Mitas, M., Cole, D.J., and Gillanders, W.E. (2003). Molecular detection of breast cancer cells in the peripheral blood of advanced-stage breast cancer patients using multimarker real-time reverse transcription-polymerase chain reaction and a novel porous barrier density gradient centrifugation technology. Clin. Cancer Res. *9*, 4865–4871.

29. Shen, Z., Wu, A., and Chen, X. (2017). Current detection technologies for circulating tumor cells. Chem. Soc. Rev. *46*, 2038–2056. https://doi.org/10.1039/c6cs00803h.

30. Gascoyne, P.R.C., Noshari, J., Anderson, T.J., and Becker, F.F. (2009). Isolation of rare cells from cell mixtures by dielectrophoresis. Electrophoresis *30*, 1388–1398. https://doi.org/10.1002/elps.200800373.

31. Chen, W., Weng, S., Zhang, F., Allen, S., Li, X., Bao, L., Lam, R.H.W., Macoska, J.A., Merajver, S.D., and Fu, J. (2013). Nanoroughened surfaces for efficient capture of circulating tumor cells without using capture antibodies. ACS Nano *7*, 566–575. https://doi.org/10.1021/nn304719q.

32. Fan, X., Jia, C., Yang, J., Li, G., Mao, H., Jin, Q., and Zhao, J. (2015). A microfluidic chip integrated with a high-density PDMS-based microfiltration membrane for rapid isolation and detection of circulating tumor cells. Biosens. Bioelectron. *71*, 380–386. https://doi.org/10.1016/j.bios.2015.04.080.

33. Lin, L., and Chung, C.K. (2021). PDMS microfabrication and design for microfluidics and sustainable energy application: review. Micromachines *12*, 1350. https://doi.org/10.3390/mi12111350.

34. Keshtiban, M.M., Zand, M.M., Ebadi, A., and Azizi, Z. (2023). PDMS-based porous membrane for medical applications: design, development, and fabrication. Biomed. Mater. *18*. https://doi.org/10.1088/1748-605X/acbddb.

35. Ji, Y., Zhang, M., Guan, K., Zhao, J., Liu, G., and Jin, W. (2019). High-performance CO_2 capture through polymer-based ultrathin membranes. Adv. Funct. Mater. *29*, 1900735. https://doi.org/10.1002/adfm.201900735.

36. Rosenbaum, M.W., Cauley, C.E., Kulemann, B., Liss, A.S., Castillo, C.F.D., Warshaw, A.L., Lillemoe, K.D., Thayer, S.P., and Pitman, M.B. (2017). Cytologic characteristics of circulating epithelioid cells in pancreatic disease. Cancer Cytopathol. *125*, 332–340. https://doi.org/10.1002/cncy.21841.

37. Mascalchi, M., Maddau, C., Sali, L., Bertelli, E., Salvianti, F., Zuccherelli, S., Matucci, M., Borgheresi, A., Raspanti, C., Lanzetta, M., et al. (2017). Circulating tumor cells and microemboli can differentiate malignant and benign pulmonary lesions. J. Cancer *8*, 2223–2230. https://doi.org/10.7150/jca.18418.

STAR★METHODS

KEY RESOURCES TABLE

REAGENT or RESOURCE	SOURCE	IDENTIFIER
Antibodies		
anti-CD45	Abcam	Cat# ab40763 RRID:AB_726545
anti-CK18	Abcam	Cat# ab93741 RRID:AB_10562119
Chemicals, peptides, and recombinant proteins		
PDMS	Shanghai Resin Factory Co., Ltd. (China)	9016-00-6
TEOS	Macklin	CAS 78-10-4
DBTDL	Aladdin	CAS 77-58-7
N-heptane	Yonghua Chemical Co. Ltd. (China)	CAS 142-82-5
Critical commercial assays		
CCK-8 kit	Dojindo, Japan	CK04
Experimental models: Celllines		
Panc-1	ATCC	CRL-1469™
Miapaca-2	ATCC	CRL-1420™
BxPC-3	ATCC	CRL-1687™
CFPAC-1	ATCC	CRL-1918™

RESOURCE AVAILABILITY

Lead contact

Further information and requests for resources and reagents should be directed to and will be fulfilled by the lead contact, Jiahua Zhou (zhoujh@seu.edu.cn).

Materials availability

This study did not generate unique reagents.

Data and code availability

- Data reported in this paper will be shared by the lead contact upon request.
- This paper does not report original code.
- Any additional information required to reanalyze the data reported in this paper is available from the lead contact upon request.

EXPERIMENTAL MODEL AND SUBJECT DETAILS

Ethics statement

Human whole blood was obtained from Zhongda Hospital Southeast University (Nanjing, China). The study protocol was approved by the Ethical Review Board of Investigation in Human Being of Zhongda Hospital Southeast University, and informed consent was obtained from all individual participants.

Chemical reagents and cell culture

PDMS was purchased from Shanghai Resin Factory Co., Ltd. (China). Tetraethyl orthosilicate (TEOS) and dibutyltin dilaurate (DBTDL) were purchased from Macklin and Aladdin, respectively. N-heptane was purchased from Yonghua Chemical Co. Ltd. (China). The nylon substrate was purchased from Millipore. Four different kinds of human pancreatic cancer cell lines, Panc-1, Miapaca-2, BxPC-3 and CFPAC-1 (all from American Type Culture Collection, Manassas, Virginia, USA), were selected as target cells and cultivated in Dulbecco's modified Eagle's medium (DMEM) (GIBCO® Invitrogen, Carlsbad, CA, USA) with 10% fetal bovine serum (GIBCO). All these cells were cultured at 37°C saturated humidity in a humidified incubator (Thermo Fisher Scientific Inc., Waltham, MA, USA) with 5% CO_2. Before each experiment, these cells were trypsinized with 0.25% trypsin and resuspended in phosphate-buffered saline (PBS) or healthy human peripheral blood. Manual counting of cells by a cell counter was repeated at least three times to account for manipulation errors.

Preparation of homoporous PDMS membranes

PDMS (10 wt%) containing 1 wt% TEOS and 0.1 wt% DBTDL was prepared as the casting solution. Cross-linking was achieved by the reaction of raw 10% PDMS, TEOS as the cross-linker, and DBTDL as the catalyst. This reaction can take place at room temperature under mild conditions. As shown in Figure S1A, when the membrane was fixed in the filtration device, the casting solution was injected into the top container of the device. Then, the vacuum pump was switched on to produce the vacuum force to drive the solution permeation into the membrane substrate. According to the top-view image (Figure S1B), the effective area of the membrane is 28.26 cm^2. The actual area of the prepared membrane in the portable blood filtration device is 1.33 cm^2. The viscosity of the PDMS solution can be controlled by the cross-linking time. Subsequently, 10 mL of the prepared solution was filtered through a nylon matrix to obtain a PDMS membrane with a specific pore size. For comparison, PDMS solutions cross-linked for different times were filtered through the nylon substrate by vacuum force. Dip-coating and spin-coating methods were also performed for membrane formation by using the same amount of PDMS solution prepared at 3 h (8.4 cP viscosity).

Cell separation

The collected human peripheral blood samples were generally filtered and separated within 4–6 hours. Before each filtration operation, a 1 mL human blood sample was taken, and 6 mL of specific lysis buffer was added for red blood cell lysis. The samples were mixed thoroughly for 8 minutes and shaken by inversion every 2 minutes. Then, the sample was transferred into the upper module of the microfilter device by a pipette gun, and the bottom module was connected to a 9 mL EDTA tube for filtration. When the level of filtered sample was about to reach the PDMS filter membrane, an additional 1 mL of PBS solution was filtered to remove the red blood cell debris from the filter. After the operation was completed, the upper module and the bottom module were separated, and the PDMS filter membrane was removed for follow-up research.

METHOD DETAILS

Cell counting kit-8 (CCK-8) assay

Four types of pancreatic cancer cells were seeded in 96-well plates at approximately 3000 cells/well. Each plate was divided into a control group and an experimental group. In the experimental group, we placed the same size PDMS filter membrane into the well. At least 5 replicate wells were used in each group. After culturing in a cell incubator at 37°C, 5% CO$_2$ and 100% humidity for 24 h, 48 h and 72 h, the cell proliferation was determined according to the recommended procedures of the CCK-8 kit (Dojindo, Japan): 10 μL CCK-8 was added to each well (CCK-8: incomplete medium = 1:9) and incubated at 37°C for another 2 h; the instrument was adjusted with blank wells, and the microplate reader was used to measure the absorbance of each well at a wavelength of 450 nm. Taking the detection time as the horizontal axis and the absorbance value as the vertical axis, the growth curve (OD450) of pancreatic cancer cells was drawn, and the growth rates of tumor cells in each group were compared.

Identification of the isolated CTCs

Then, anti-CD45 antibody (Abcam, USA) was added to the filter membrane and incubated at 4°C for 30 min. After washing with 100 μL of PBS, 0.2% Triton X-100 was added to the filter membrane and incubated for 10 minutes to permeate the membrane. The purpose of permeabilization is to enable the filter membrane to be stained by anti-CK18 antibody (Abcam, USA). After permeabilization, the filter membrane was rinsed with 100 μL of PBS to remove excess staining solution. 4,6-Diamino-2-phenylindole (DAPI) was added to the filter membrane at 37°C for 30 min. Finally, 4% paraformaldehyde (PFA) was added to the filter membrane to fix the entrapped cells, and the membrane was rinsed with PBS to remove residual reagents. After all operations, the captured cells were identified and counted under a fluorescence microscope. Cytokeratin 18-positive (CK18$^+$, red), 4,6-diamino-2-phenylindole-positive (DAPI$^+$, blue) and CD45-negative (CD45$^-$) cells were CTCs. White blood cells were negative for CK18 (CK18$^-$) and positive for CD45 (CD45$^+$, green).

QUANTIFICATION AND STATISTICAL ANALYSIS

All data are presented as the mean ± SD. Statistical analysis of the data was performed with SPSS (SPSS Inc., Chicago, IL, United States; version 22.0) using one-way ANOVA or the unpaired Student's t test. $p < 0.05$ was regarded as statistically significant.